

## Geochemical, mineralogical and macroscopic facies of the Fongo-Tongo bauxite deposit western Cameroon

Franck Wilfried Nguimatsia Dongmo , Rose Yongue Fouateu , Roger Firmin Donald Ntouala , Yanick Brice Lemdjou , Dongmo Chirstophe Ledoux & Anthony Temidayo Bolarinwa

To cite this article: Franck Wilfried Nguimatsia Dongmo , Rose Yongue Fouateu , Roger Firmin Donald Ntouala , Yanick Brice Lemdjou , Dongmo Chirstophe Ledoux & Anthony Temidayo Bolarinwa (2021): Geochemical, mineralogical and macroscopic facies of the Fongo-Tongo bauxite deposit western Cameroon, Applied Earth Science, DOI: [10.1080/25726838.2020.1861916](https://doi.org/10.1080/25726838.2020.1861916)

To link to this article: <https://doi.org/10.1080/25726838.2020.1861916>



Published online: 20 Jan 2021.



Submit your article to this journal [↗](#)



View related articles [↗](#)




View Crossmark data [↗](#)

---



## Geochemical, mineralogical and macroscopic facies of the Fongo-Tongo bauxite deposit western Cameroon

Franck Wilfried Nguimatsia Dongmo <sup>a,b,e</sup>, Rose Yongue Fouateu<sup>b</sup>, Roger Firmin Donald Ntoulala<sup>a,b</sup>, Yanick Brice Lemdjou<sup>c</sup>, Dongmo Christophe Ledoux<sup>d</sup> and Anthony Temidayo Bolarinwa<sup>e</sup>

<sup>a</sup>Department of Mining Engineering and Mineral Processing, Faculty of Mines and Petroleum Industries, University of Maroua-Cameroon, Kaele, Cameroon; <sup>b</sup>Department of Earth Sciences, University of Yaounde 1, Yaounde, Cameroon; <sup>c</sup>School of Earth Sciences and Resources, China University of Geosciences, Beijing, People's Republic of China; <sup>d</sup>Geothermal Science and Technology, Institute of Applied Geosciences, Technical University of Darmstadt, Darmstadt, Germany; <sup>e</sup>Department of Geology, Pan African University, Life and Earth Sciences Institute (PAULESI), University of Ibadan, Ibadan, Nigeria

### ABSTRACT

The Fongo-Tongo's bauxites were investigated to characterise them. Their texture varies from massive, vesicular, alveolar, conglomeratic to nodular with dominantly red colour, reddish-brown and yellow. The main minerals identified by X-ray diffraction are gibbsite and goethite with subordinate quartz, anatase, hematite, magnetite, and traces of kaolinite. The abundance of gibbsite and goethite suggested intense weathering during the formation of the bauxite deposits. Chemical data of the bauxite showed high Al<sub>2</sub>O<sub>3</sub> (37.4–57.5 wt-%) with varied Fe<sub>2</sub>O<sub>3</sub> (3.97–29.5 wt-%), TiO<sub>2</sub> (0.57–7.5 wt-%) and SiO<sub>2</sub> (0.48–3.21 wt-%) contents, while other oxides are generally less than 0.6 wt-% indicating high bauxite quality with low impurities. The wide range of trace and REE concentrations of Zr, Nb, Sr, V, Ce, La, Nd and the presence of both positive and negative Eu anomalies suggested and acid igneous source with mafic input. These bauxites could serve as raw material for the aluminium industry.

### ARTICLE HISTORY

Received 26 June 2020  
Revised 13 November 2020  
Accepted 3 December 2020

### KEYWORDS

Texture; mineralogy; geochemistry; weathering; lateritic bauxites; aluminium industry; igneous source; Fongo-Tongo

## Introduction

Bauxite, a whitish to reddish-brown lateritic regolith, characterised by high content of alumina (Al<sub>2</sub>O<sub>3</sub>) and iron oxides (Fe<sub>2</sub>O<sub>3</sub>) constitutes the principal ore for the production of aluminium. Bardossy (1982) defines bauxite as a rock in which aluminous minerals constitute more than half the weight. A combination of oxides and hydroxides of iron, titanium and aluminium was regarded as bauxite by Tardy (1993). Bauxite, the primary source of aluminium, represents a typical accumulation of weathered materials from the continental crust (Valeton 1972). Bauxite is used to determine paleoclimates (Bardossy and Aleva 1990; Price et al. 1997; Bardossy and Combes 1999) because it records various climatic, biological, pedogenetic and paleoenvironmental conditions (Valeton 1999). High temperatures, humidity and precipitation are widely regarded as the main conditions for its formation (Akayemov et al. 1975; Tardy et al. 1991).

There are two main genetic groups of bauxite deposits in the world namely karstic bauxites overlying carbonate rocks and lateritic bauxites generated from aluminosilicate rocks (Bardossy 1982). While karst-type deposits originate from a wide range of materials, depending on the source area (Bardossy 1982), lateritic bauxite is generally through in-situ

lateritisation, hence, the major factors that determine the extent and grades of bauxite are the parent rock composition, climate, topography, drainage, groundwater chemistry and movement, location of the water table, microbial activity and the duration of weathering processes (Bardossy and Aleva 1990; Price et al. 1997). The lateritic bauxites features are usually directly related to the underlying source rocks associated textures and compositions (Bardossy and Aleva 1990). The Cameroon Volcanic Line offers the distinction of being one of the few magmatic entities which developed in oceanic and continental areas. Sato et al. (1990) showed that the mainland can be further subdivided into monogenic (plains of Tombel, Kumba, Noun and Mount Oku) and polygenic land (Mounts Cameroon, Manengouba, Bambouto and the Bamenda highlands).

Worldwide, nearly 85% of reserves are of the lateritic type and occupy large areas, mainly in the intertropical zone (Ségalen 1964).

Bauxite is one of the primary raw materials used by heavy industries. The increasingly growing demand for high-grade bauxite for the development and production of quality refractory materials used in the construction of furnaces and reactors or the construction of incinerators for the treatment of

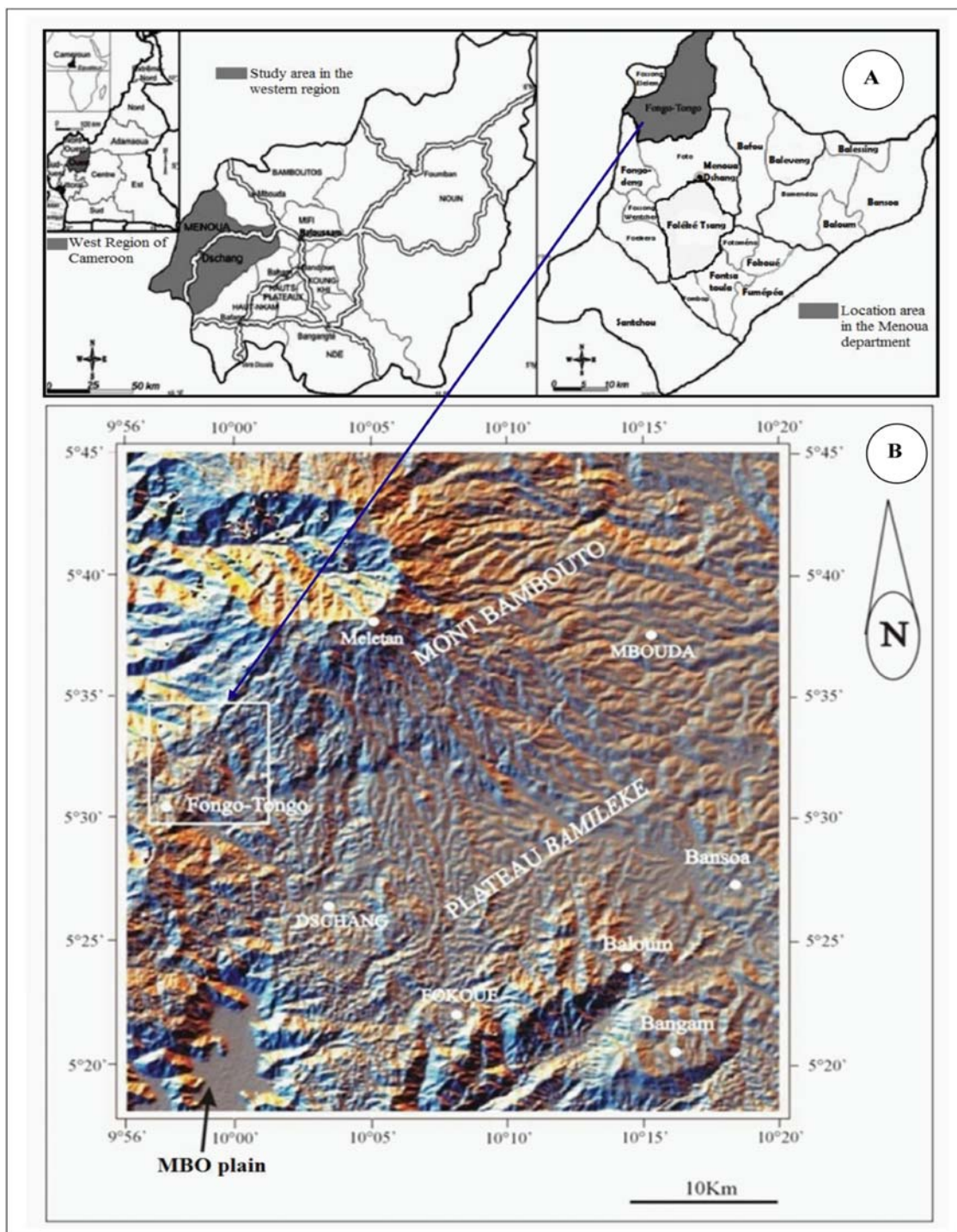


**Figure 1.** Location of Fongo-Tongo area (a) on the administrative map of Menoua (b) on the SSW flank of Mount Bambouto.

solid waste has necessitated the exploration for newer deposits to meet this growing demand. Lateritic bauxite is the main type of bauxite present in Cameroon (Belinga 1972; Momo Nouazi et al. 2012; Nguimatsia et al. 2019). Important deposits are found in the Adamawa plateau (Minim-Martap, Ngaoundal) and Western highland (Fongo-Tongo, Bangam) (Belinga 1972; Nyobe 1987). Occurrences of bauxite have also been reported in Fokamezou-Doumbouo-Fokoué in SSE of Dschang and locality of Bangam (Laplaine 1969; Momo Nouazi et al. 2012). Characterisations carried out on these

different deposits are presented in Appendix 1. Although the Fongo-Tongo bauxite constitutes the largest western Highlands' deposit, it appears to be less investigated compared to other bauxite deposits. Hence, detailed knowledge of the geological and geomorphological settings, mineralogy as well as the geochemistry of the Fongo-Tongo lateritic bauxite occurrences seems imposed. The present work's major objective therefore lies in investigating the Fongo-Tongo bauxite; associated mineralogical and geochemical facies, to identify the ores' precursor by means of the major and trace elements'

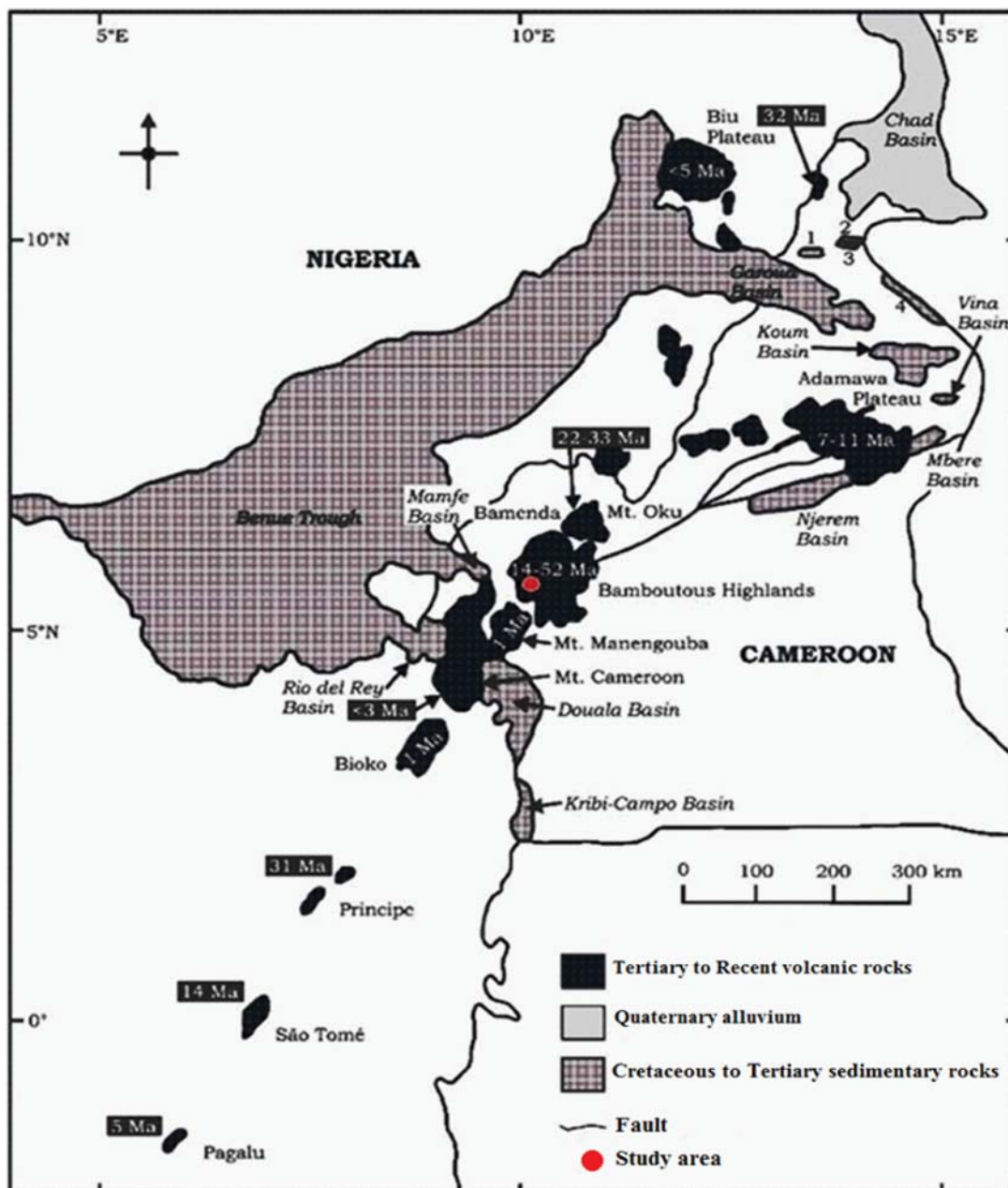


**Figure 2.** The location of Fongo-Tongo area within the Cameroon Volcanic Line (CVL) (modified after Njonfang et al. 2011).

distribution, along with the deposits relating comprehensive geological, mineralogical and geochemical characterisation.

### Geological setting

Geographically, the study area is located on the SSW flank of Mont Bamboutos, between longitudes E09 ° 57' to E10 ° 01' and latitude N05 ° 30' to N5 ° 35' (Figure 1).

The Bamboutos massif to which the study area belongs is a huge volcanic shield of roughly elliptical shape belonging to the Cameroon volcanic line, CVL (Figure 2).

The CVL is an N030°E alignment of oceanic and continental volcanic mountains, and anorogenic

plutonic complexes, extending from Pagalu Island to Lake Chad (Déruelle et al. 1991). Magmatic activity along this line began 65 Ma ago (Njonfang et al. 2011). It is embodied in the oceanic part by four islands in the Gulf of Guinea (Pagalu, Sao Tome, Principe and Bioko) and on the mainland by the volcanic massifs (Mounts Cameroon, Rumpi, Manengouba, Bambouto and Oku).

### Local geology

The Fongo-Tongo area is within the Bambouto massif which is a polygenic complex composite volcano (Morin 1988). Four main rock groups, namely felsic, mafic, pyroclastic rocks and basement granitic-gneiss were reported by many workers (including Tchoua 1974; Youmen 1994 and Nni and Nyobe 2011).

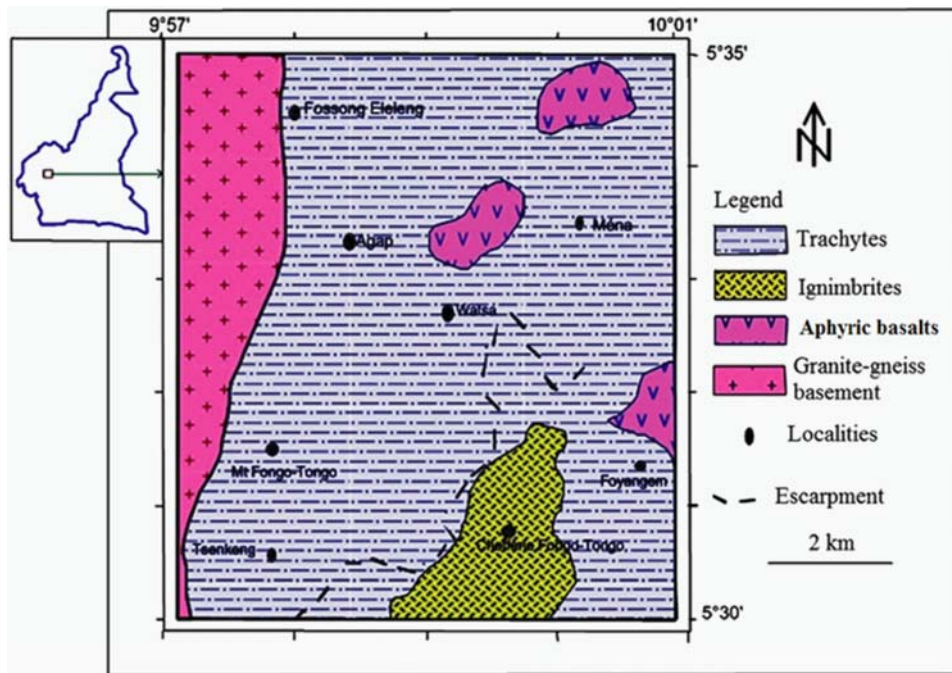


Figure 3. Geologic map of the study area (after Nguimatsia 2013).

The felsic rock consists of trachyte (Nni and Nyobe 2011), which is widespread in the northern part and covering more than 75% of this area (Figure 3). Outcrops of trachyte occur as grey to dark-grey volcanic rock mass. The mafic rocks are alkali basalts and basanites (Nni and Nyobe 2011). They occur as porphyritic dark-grey to black, massive volcanic rocks in the southern part of the massif and as islets species embedded in trachytic napes covering about 10% of

the study area. The pyroclastic rocks also outcrop in the southern part of the study area, around Fongo-Tongo palace. They occupy about 5% of the study area. They are intensely altered rocks of dominantly trachytic compositions (Figure 3). Crystalline basement outcrop east of the study area where they form a North–South band of about 1.5 km long (Figure 3). They constitute about 15% of the study area and consist of intrusive granites and gneisses (Dumort 1968).

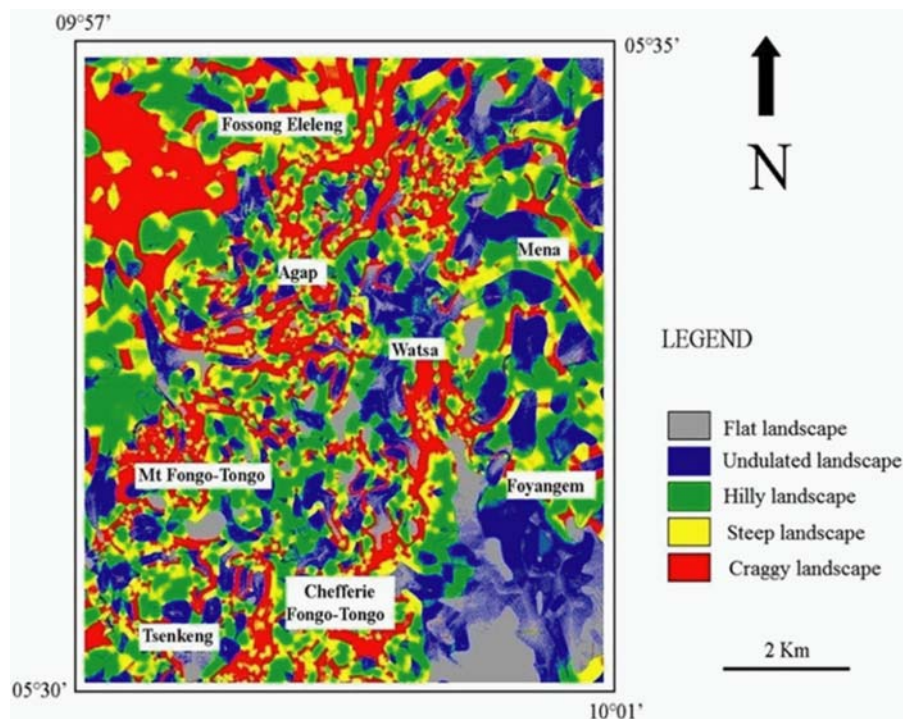
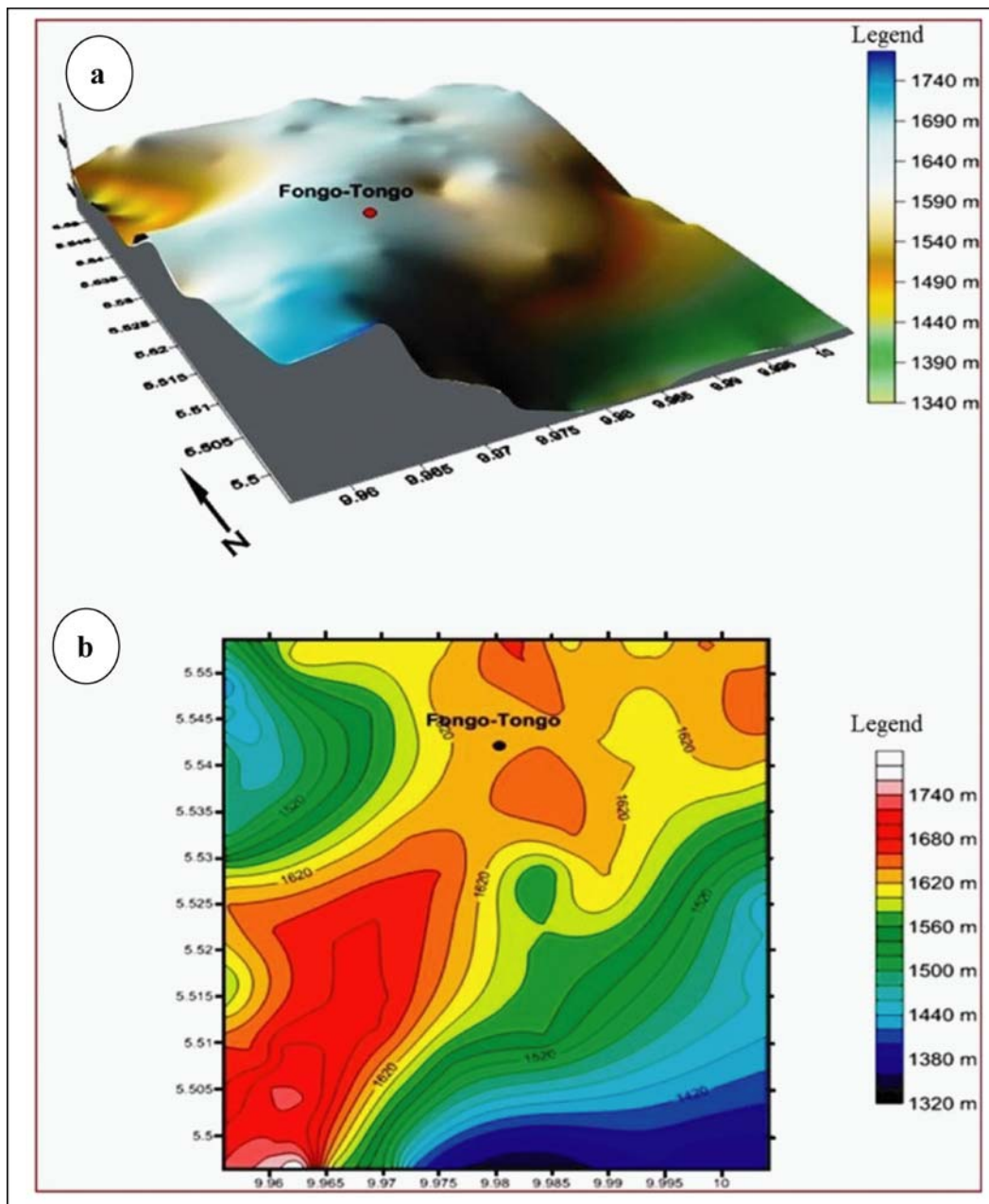


Figure 4. Slopes map of study area.



**Figure 5.** Geomorphology of the Fongo-Tongo area showing (a) 3D view of the relief and (b) morphologic units map (after Ngui-matsia 2013).

### Geomorphology

The Fongo-Tongo area occurs on the southern flank of the volcanic massif of Mount Bambouto (Figure 1). It is characterised by a gentle undulating to flat relief. According to Belinga (1972), these surfaces are topographic features that have been subjected to erosion and tectonics activities. The five morphological units identified in the area include flat landscape, undulated landscape, hilly landscape, steep landscape and craggy landscape (Figure 4).

- a. The flat landscape (Figure 4) consists of slopes of less than  $2^\circ$  and covers approximately 8% of the study area. These are outliers of landscape next to the undulating or hilly landscape above

1600 m altitude. They occur to the southeast of the study area.

- b. The undulated landscape (Figure 4) occurs as slopes of between  $2^\circ$  and  $5^\circ$ . It occupies approximately 28% of the study area. These are outliers of landscapes next to hilly and steep landscapes. It is adjacent to the flat landscape and extends to the southeast of the study area.
- c. The hilly landscape (Figure 4) consists of slopes of between  $5^\circ$  and  $10^\circ$ . It occupies about 23% of the area and is intimately linked to the hanged landscape, which forms the watershed line.
- d. The steep landscapes are made up of slopes ranging from  $10^\circ$  to  $15^\circ$ . They occupy about 15% of the area and consist of small shreds of landscapes generally spread over the entire area.

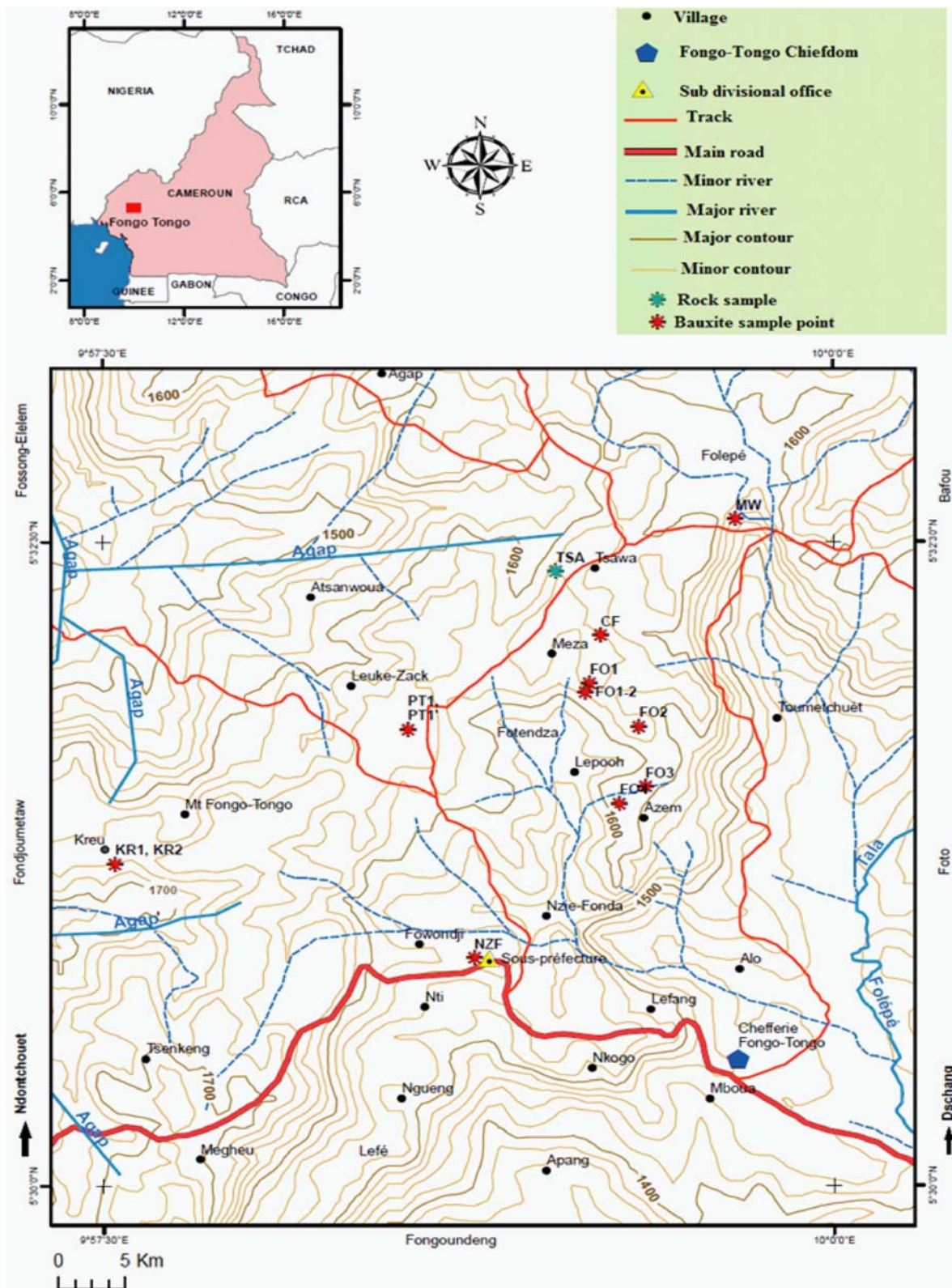


**Figure 6.** Bauxite sample location map at Fongo-Tonga area.

e. The craggy landscapes are made up of slopes ranging from 15° to 89°. They occupy about 15% of the study area, on the Agap – Mont Fongo-Tonga line and the open fan-shape area towards the northwest.

The relief of Fongo-Tonga area can be classified into three based on the altitudes. The low area

(1320–1440 m), average area (1500–1620 m) and zone of high altitude (more than 1700 m) (Figure 5).

### Methodology

Geological mapping and systematic sampling of bauxite was carried out in the Fongo-Tonga area (Figure 6). The representative samples selected were

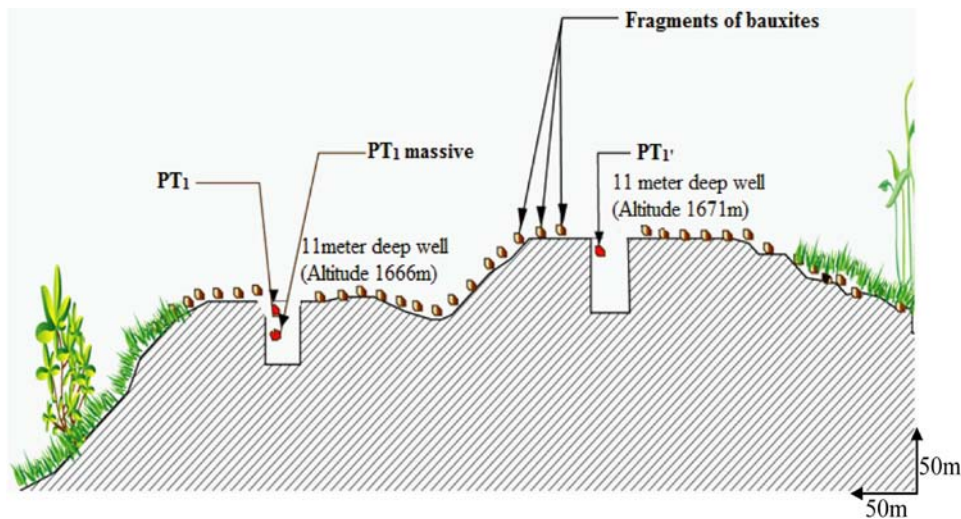


**Figure 7.** Morphology of the Leuke-zack's bauxite locality (8a = PT1; 8b = PT<sub>1massif</sub>; 8c = PT<sub>1</sub>).

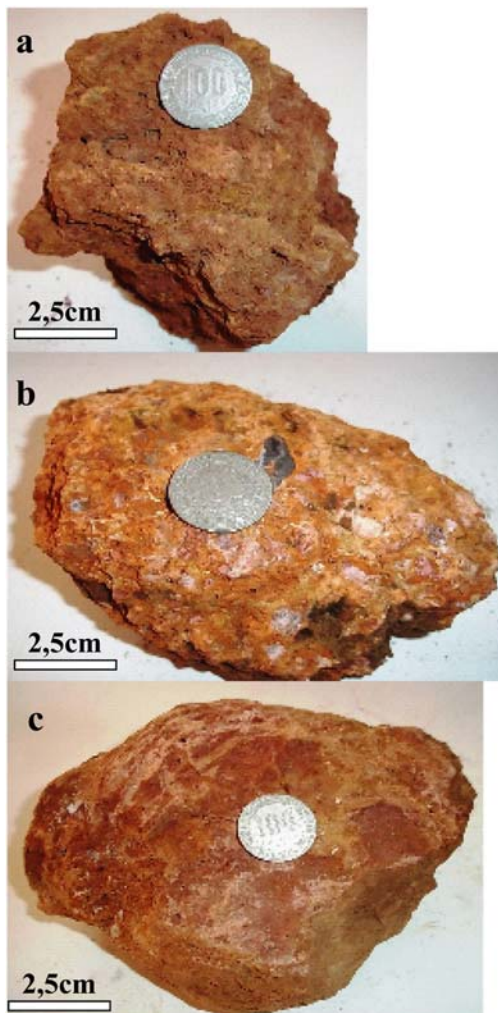


**Figure 8.** Bauxites facies observed in the Leuke-zack locality. (a) Nodular to vesicular indurated bauxite. This dense material presents sub-angular to sub-rounded rims with white spots in certain places. The nodules have sizes less 1 cm fragments. (b) Bauxite with massive facies. Very hard and dense. It has smooth rounded to sub-angular rims and it is devoid of voids. (c) Reddish-yellow dense and sub-spherical nodular material. The grey and yellow nodules are embedded in a matrix of red to yellowish-brown. The bauxite is highly indurated, with few voids.

pulverised and subjected to mineralogical and geochemical analyses. Major oxides, trace and rare-earth elements (REE) composition were determined at the ALS Chemex laboratories, South Africa. The bauxite major oxides composition was determined by weighing 0.2 g of the powdered bauxite sample into which a solution of 0.9 g lithium metaborate ( $\text{LiBO}_2$ ) and lithium tetraborate ( $\text{Li}_2\text{B}_4\text{O}_7$ ) was added, homogenised and melted in an oven at  $1000^\circ\text{C}$ . The product obtained was cooled and dissolved respectively in 100 ml of 4% and 2% nitric and hydrochloric acid. This solution was then analysed using the inductively coupled plasma-atomic emission spectroscopy (ICP-AES).

Trace elements composition was determined using 0.2 g of the powdered bauxite sample into which a solution of lithium borate (0.9 g) was added, homogenised and melted in an oven at  $1000^\circ\text{C}$ . The product obtained was cooled and dissolved in a solution of 100 ml of 4%  $\text{HNO}_3$  and 2%  $\text{HCl}$ . This solution is then analysed using the inductively coupled plasma-mass spectrometer (ICP-MS).

X-ray diffraction (XRD) analyses were carried out on the pulverised and mounted bauxite samples using the SCINTAG XDS 2000 diffractometer of the Department of Geology, University of Liege, Belgium. The instrumental settings are 40 kV, 35 mA and  $\text{CuK}\alpha$  radiation. The mineralogical identification from the diffraction patterns was carried out using Brindley and Brown (1980) and Moore and Reynolds Jr (1989).

## Results and discussions

### Description of bauxite facies

The Fongo-Tongo bauxite occurs in different locations and forms. They include eroded gravel size bauxites at the hill bottom, jointed large discontinuous



bauxites on hill summits, loose and discontinuous large bauxites on hill tops and slopes. These bauxites affect the morphology of some localities where very large bauxites blocks occur on the summit while the flanks of hills and the lower plains are characterised by basalt blocks.

### *Bauxite facies in the Leuke-zack locality*

Leuke-zack is located at coordinates E09°58'36" and N05°31'52" at an altitude of 1666 m. In this locality, the colour of bauxite varies from light yellow to grey through red and brown. The topography of Leuke-zack area is characterised by undulating, gentle and hilly landscapes. The hills are separated by lowlands (Figure 7). The bauxites facies vary from nodular-vesicular (Figure 8(a)) to massive (Figure 8(b)) and nodular (Figure 8(c)).

### *Nzie-Fonda bauxites*

The Nzie-Fonda plateau is located at an altitude of 1582 m. Its coordinates are 09°58'49"E and 05°30'53"N. On this plateau, large fragments of bauxite abound on the surface. These bauxites fragments are



**Figure 9.** Nzie-Fonda bauxite Facies. Bauxitic material with massive vermiculate facies. It has void spaces.

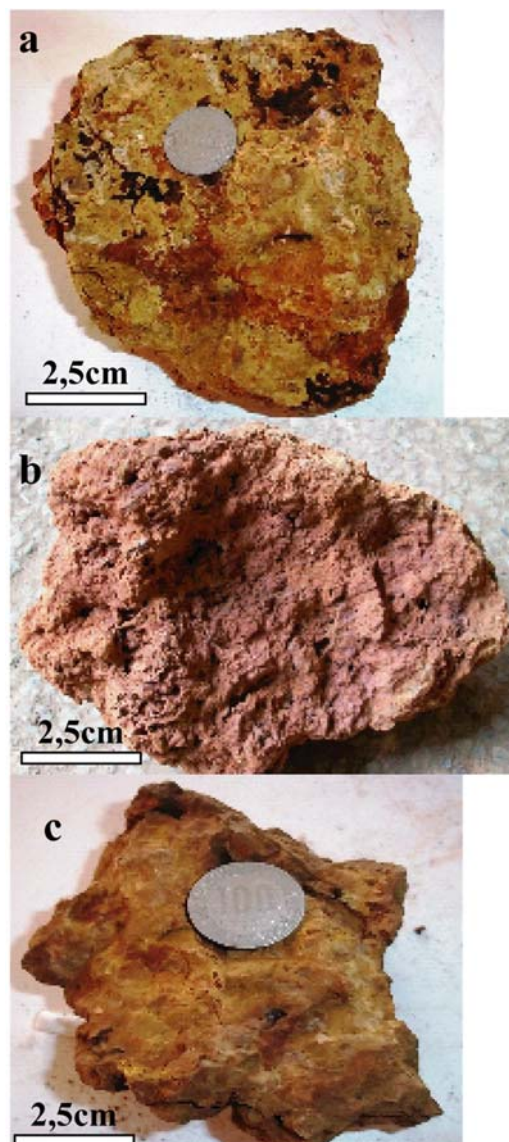


**Figure 11.** Meza bauxite Facies. (a) Nodular to vesicular facies: The bauxite has nodules of less than 1 cm. These nodules with yellow surfaces and sub-angular contours have red patches indicating oxidation of iron. (b) Alveolar bauxite facies: Reddish-brown bauxite with void spaces. They are highly indurated with red patches and small vesicles. (c) Massive bauxite: Massive and dense bauxite, with a matt surface.

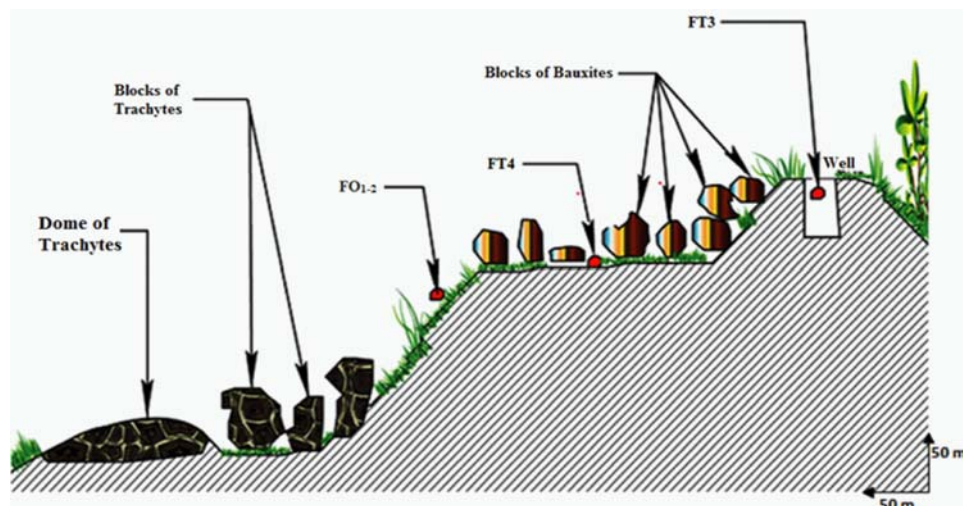


**Figure 10.** Sectional view of the Meza relief and bauxite sampling points.

yellowish-red in colour and have a massive vermicular structure (Figure 9).

### **Meza locality bauxites**

Meza is located at an altitude of 1646 m, within coordinates E9°59'20" and N5°31'47". The bauxite observed here, are outcropping in discontinuous blocks and slabs (Figure 10). They are nodular to vesicular (Figure 11(a)), alveolar (Figure 11(b)) and massive (Figure 11(c)).

### **Lepooh locality bauxites**

The Lepooh Summit is located at 1610 m altitude, with coordinates E09°59'21" and N05°31'33". The bauxites outcropping here are in blocks of variable sizes (Figure 12). Hand specimen of massive bauxite with pseudo-conglomeritic features occur in this locality. They are reddish-brown in colour.

### **Kreu locality bauxite**

The Kreu locality is located at an altitude of 1652 m altitude, with coordinates: E09°57'32" and N05°31'15". The bauxites in this locality are bright red in colour, highly indurated and massive (Figure 13).

### **Descriptions of the lateritic bauxite profiles at Fongo-Tongo area**

The Fongo-Tongo lateritic bauxite profiles (Figure 14) are similar in their characteristics from one location to another. The bauxite profile in Leuke-Zack locality, from top to bottom is described in this session (Figure 14).

The Horizon B1 ranged from 0 to 100 cm and consists of fine material and indurate elements.

The fine earth is dark red, clay-loam material (2.5YR3/6), consisting of very fine to medium blocky to lumpy structures. It is very porous and friable. The hardened elements within the horizon consist of gravel and blocks that are red in colour (10R4/6) and massive to scoriaceous. They constitute about 10% of the total volume of the horizon.

Horizon B2 ranged from 100 to 620 cm and consist of very hard, dense, reddish massive block (10R4/6) with red and yellowish streaks (5YR4/8).

Horizon B3 at 620–820 cm is made up of dark clay material and gravel. The dark clay material (2.5YR7/8) is characterised by a fine to medium blocky structure. The gravel level is less than a centimetre in thickness and dark red in colour (10R4/6) with sub-angular fragments. They constitute about 10% of the total volume of material on the horizon. They are all similar to those of the overlying B1 horizon.

Horizon C at 620–1000 cm consist of whitish grey prismatic material (2.5Y6/2), with yellowish streak (10YR5 /).

In summary, the profile showed a massive duricrust horizon (B2) sandwiched by two gravelly horizons B1 and B3. The upper gravelly horizon consists of fragments. These fragments are also present in the lower gravelly horizon.

### **Mineralogy of the Fongo-Tongo bauxites**

Fongo-Tongo bauxites exhibit variations in petrography and mineralogy. They are nodular to conglomeratic, vesicular, alveolar and vermicular. In some places around the summits due to the circulation of percolating waters in the pore spaces of the duricrusts materials, changes in facies can be observed and are



**Figure 12.** Bauxite blocks in LePooh locality.



**Figure 13.** Kreu massive bauxite facies. Smooth massive bauxite devoid of cavities.

suggestive of evolution from conglomeritic to a nodular facies. Whereas, on the flanks or hills, the observed vesicular, alveolar and vermicules facies of these materials can be attributed to the dismantling and more pronounced alteration of the initial massive duricrusts (Boulangé 1984). It has been shown by Hiéronymus (1973) that cortex around nodules could be formed by speleothems or centripetal alteration. The

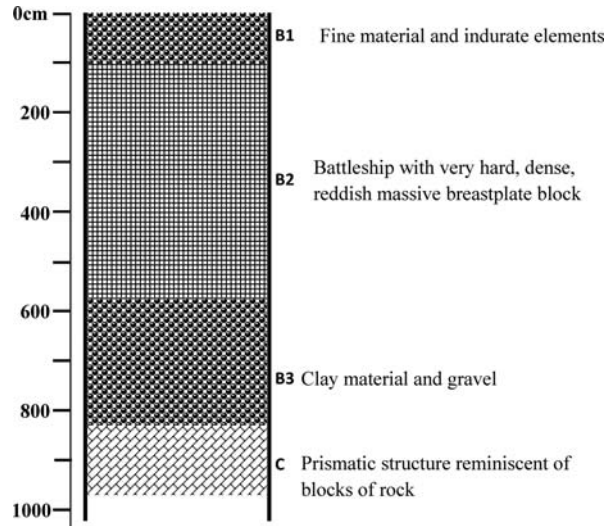


**Figure 14.** Fongo-Tongo lateritic bauxite profiles.

duricrusts have variation in colours. The most prominent colours of the bauxites are red, brick red, reddish brown, brown, pink, yellow and ochre. However, some have spots and purple textures with greenish mottling.

Bauxites with red colours have been described by Grubb and PLC (1973) in Australia and by

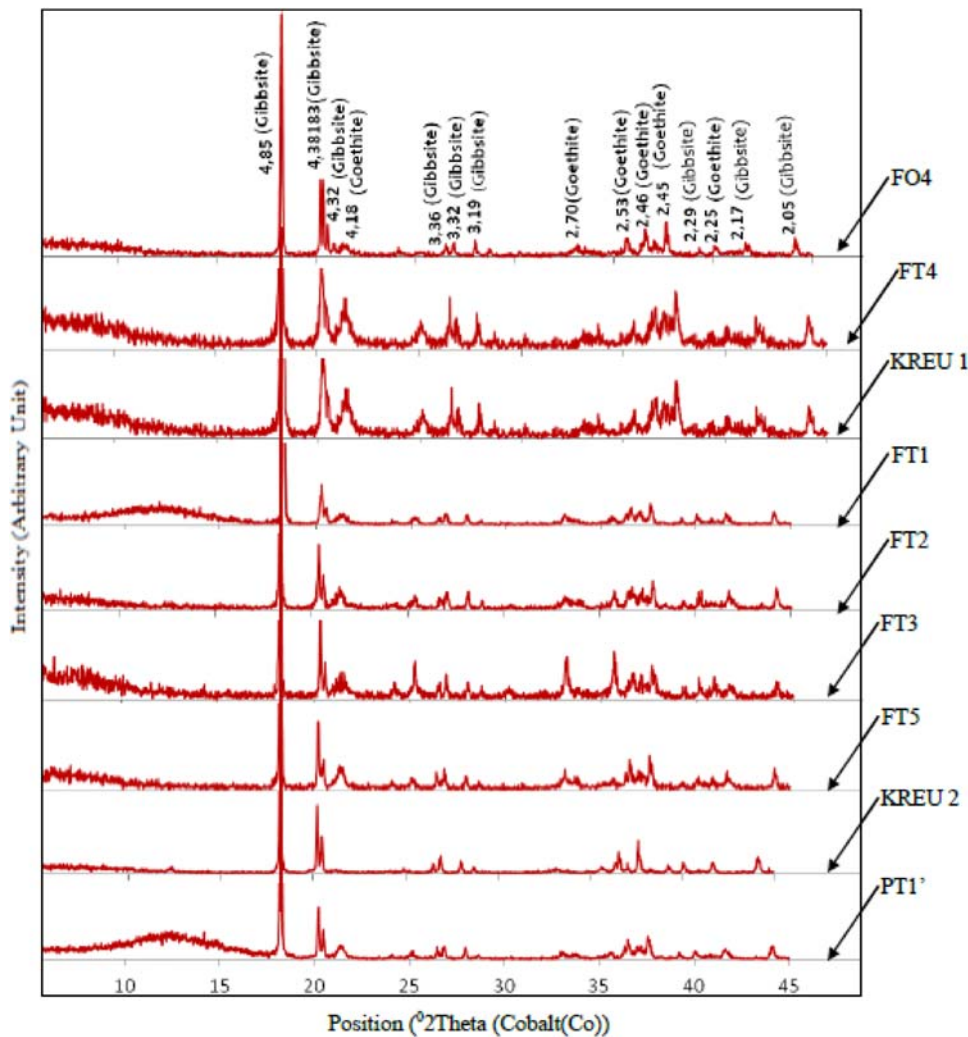


**Figure 15.** X-ray Diffractograms of Fongo-Tongo bauxite samples (FO4, FT4, KREU1, FT1, FT2, FT3, FT5, KREU2 and PT1').

**Table 1.** Mineralogical composition of the Fongo-Tongo bauxite.

Samples	Minerals						
	Anatase	Gibbsite	Goethite	Magnetite	Quartz	Hematite	Kaolinite
F04		+++	++				
FT1		++++	+++				
FT2		++++	+++		+		
FT3		++++	++++	+		+	
FT4	+	++++	+++				
FT5		++++	+++				
Kreu1		++++	+				+
Kreu2		++++	+++				+
PT1'		++++	+++				+

Legend: ++++ = very abundant, +++ = Abundant, ++ = moderately abundant, + = Trace.

**Table 2.** Major oxide compositions (%), trace and rare-earth elements (ppm) of Fongo-Tongo bauxites.

		FT4	FT2	FT3	FT5	KREU1	F04	PT1'	FT4
SiO <sub>2</sub>	0.01	2.39	1.03	0.48	1.03	3.21	1.21	1.06	2.39
Al <sub>2</sub> O <sub>3</sub>	0.01	44.0	48.2	37.4	49.4	57.5	49.8	51.6	44.0
Fe <sub>2</sub> O <sub>3</sub>	0.01	17.50	14.95	29.3	16.75	3.97	19.30	12.85	17.50
MgO	0.01	0.10	0.03	0.21	0.02	0.01	0.01	0.02	0.10
MnO	0.01	0.04	0.04	0.07	0.03	<l.d	0.03	0.03	0.04
TiO <sub>2</sub>	0.01	3.93	2.15	7.47	2.23	0.57	1.65	2.01	3.93
K <sub>2</sub> O	0.01	0.01	0.01	<l.d	0.01	0.01	0.01	0.01	0.01
Na <sub>2</sub> O	0.01	<l.d	0.01	0.01	0.01	0.01	0.01	0.01	<l.d
CaO	0.01	0.01	<l.d	0.02	<l.d	<l.d	<l.d	0.01	0.01
P <sub>2</sub> O <sub>5</sub>	0.01	0.37	0.15	0.53	0.13	0.05	0.24	0.10	0.37
Cr <sub>2</sub> O <sub>3</sub>	0.01	0.06	0.02	0.16	0.01	<l.d	0.01	0.03	0.06
LOI	0.01	29.3	30.1	24.5	29.1	31.3	29.3	31.2	29.3
Total	-	97.72	96.7	100.16	98.73	96.66	101.58	98.93	97.72
Traces elements (ppm)									
Sc	1	1	13	7	28	7	6	10	9
V	5	5	425	136	667	102	8	94	117
Ga	0.1	0.1	43.4	59.7	48.9	95.9	31.0	55.7	76.8
Sr	0.1	0.1	137.0	32.2	345	16.3	0.7	18.7	16.5
Y	0.5	0.5	20.8	20.4	44.7	32.1	24.6	12.5	39.3
Zr	2	2	504	1210	599	2310	923	1035	1825
Nb	0.2	0.2	125.0	215	180.5	350	104.0	162.5	289
Ba	0.5	0.5	80.2	47.2	154.0	28.2	2.6	28.7	25.5
Hf	0.2	0.2	12.5	30.3	14.4	57.0	21.2	24.9	46.2
Ta	0.1	0.1	7.7	13.9	9.0	15.0	6.2	9.4	12.2
Sn	1	1	4	9	5	13	3	5	10
Th	0.05	0.05	16.25	21.7	14.45	42.0	9.78	15.80	35.8
U	0.05	0.05	4.89	5.25	5.14	8.00	2.35	4.86	7.23
W	1	1	2	3	2	4	2	2	5
Cd	0.5	0.5	5.0	3.1	6.9	3.4	0.5	4.1	3.1
Co	1	1	5	<l.d	10	<l.d	<l.d	<l.d	<l.d
Cu	1	1	15	3	16	4	2	4	1
Mo	1	1	6	12	7	22	2	8	12
Ni	1	1	8	<l.d	16	<l.d	3	<l.d	<l.d
Pb	2	2	16	16	23	10	<l.d	5	8
Zn	2	2	36	55	72	29	8	77	30
Cr	10	10	520	110	980	80	10	70	150
Cs	0.01	0.01	0.03	0.01	<l.d	<l.d	<l.d	0.01	<l.d
Rb	0.2	0.2	0.5	0.4	<l.d	<l.d	0.2	<l.d	0.3
Tl	0.5	0.5	<l.d	<l.d	<l.d	<l.d	<l.d	<l.d	<l.d
Ag	0.5	0.5	<l.d	05	<l.d	0.8	<l.d	<l.d	0.7
As	5	5	18	11	13	10	<l.d	8	15
Rare-earth elements (ppm)									
La	0.5	72.3	440	144.00	233	2.4	24.7	22.7	72.3
Ce	0.5	129.0	162.5	239	137.0	24.9	99.2	136.5	129.0
Pr	0.03	14.10	7.51	33.7	4.16	0.77	4.75	4.00	14.10
Nd	0.1	48.7	24.8	126.5	13.4	3.1	16.1	13.2	48.7
Sm	0.03	8.41	4.61	24.5	3.52	1.45	3.02	3.57	8.41
Eu	0.03	2.92	1.33	9.12	0.90	0.39	0.74	1.06	2.92
Gd	0.05	7.46	4.44	22.9	4.17	1.99	2.89	4.67	7.46
Tb	0.01	1.00	0.74	2.89	0.87	0.55	0.45	1.04	1.00
Dy	0.05	5.31	4.48	13.65	6.00	4.75	2.82	7.23	5.31
Ho	0.01	0.97	0.92	2.13	1.41	1.12	0.61	1.63	0.97
Er	0.03	2.36	2.72	4.06	4.21	3.54	1.50	5.00	2.36
Tm	0.01	0.32	0.47	0.44	0.75	0.64	0.26	0.90	0.32
Yb	0.03	2.07	3.25	2.10	5.51	4.85	1.96	6.22	2.07
Lu	0.01	0.26	0.46	0.25	0.76	0.71	0.23	0.87	0.26
ΣREE		295.18	262.23	625.24	205.96	51.16	159.23	208.59	295.18
ΣLREE		275.43	244.78	576.82	182.28	33.01	148.51	181.03	275.43
ΣHREE		19.75	17.48	48.42	23.68	18.15	10.72	27.56	19.75

(Continued)

**Table 2.** Continued.

	FT4	FT2	FT3	FT5	KREU1	F04	PT1'	FT4
LREE/HREE	13.95	14.00	11.91	7.70	1.82	13.85	6.57	13.95
Ce/Ce*	0.98	2.17	0.83	3.37	4.44	2.22	3.47	0.98
Eu/Eu*	0.18	0.19	0.11	0.16	0.22	0.20	0.16	0.18
(La/Yb) <sub>N</sub>	23.73	9.20	46.58	2.87	0.34	8.56	2.48	23.73

L.d = Detection Limite.

LOI = Loss on ignition.

$Ce/Ce^* = (Ce_{sample}/Ce_{chondrite}) / [(La_{sample}/La_{chondrite})^{1/2} (Pr_{sample}/Pr_{chondrite})^{1/2}]$ .

$Eu/Eu^* = (Eu_{sample}/Eu_{chondrite}) / [(Sm_{sample}/Sm_{chondrite})^{1/2} (Gd_{sample}/Gd_{chondrite})^{1/2}]$ .

$(La/Yb)_N = (La_{sample}/La_{chondrite}) / (Yb_{sample}/Yb_{chondrite})$ .

Hiéronymus (1973) and Nyobe (1987) in Cameroon. Their red colouration is due to the presence of iron in the form of hematite (Ségalen 1964; Schwertmann and Murad 1983). The yellow matrix inside most of these materials from Fongo-Tongo could result from deferruginisation of bauxite originally reddish in colour. This type of insitu alteration of laterite has been described by Yongue Fouateu (1986) in the ferruginous duricrusts of Yaoundé.

The mineralogical composition determined from XRD showed dominant gibbsite and goethite peaks (Figure 15), with traces of quartz, anatase, maghemite, hematite and kaolinite (Table 1). Prominent gibbsite peaks occur at 4.85, 4.38, 4.32, 3.36, 3.32 and 3.19 Å. Goethite peaks are recorded at 4.18, 2.70, 2.53, 2.46, 2.45 and 2.25 Å.

### Geochemistry of the Fongo-Tongo bauxite

The chemical composition of the Fongo-Tongo bauxite is presented in Table 2. The data showed high Al<sub>2</sub>O<sub>3</sub> (37.4–57.5 wt-%) and loss on ignition (LOI) (24.5–31.3 wt-%). The Fe<sub>2</sub>O<sub>3</sub> varied from 3.97 to 29.5 wt-%, TiO<sub>2</sub> 0.57–7.5 wt-% and SiO<sub>2</sub> 0.48–3.21 wt-%. Other oxides are generally less than 0.6 wt-% indicating high bauxite quality with very low impurities. The trace and rare-earth element concentrations varied widely from those characteristic of acid igneous rocks to those of mafic rocks as exemplified by Zr (504–2310), Nb (104–350), Sr (0.7–345), V (8–667), Ce (24.9–239), La (2.4–144), Nd (3.1–126) ppm. The presence of both positive and negative Eu anomalies (Figure 16(c)) suggested an acid igneous source with mafic input. The presence of anatase and probably leucosene, an alteration product of ilmenite indicated intense chemical weathering. Immobile elements (Al, Ti, Zr and Nb) enrichment during the bauxitisation process revealed the important role of this intense chemical weathering on the formation of the bauxites and the concentration of these elements within the lateritic profiles in the Fongo Tongo area.

The Fongo-Tongo bauxite displays significant concentration of zirconium (504–2310 ppm), likely associated with the presence of zircon in the parent rock. That is apart from significant concentration of trace elements, notably Sr, Ba and LREE; La, Ce, Pr and Nd relative to HREE. As noted earlier, the

geochemical data suggest that Zr, Y, Nb, Mo, V, Sc, Sr, and Ba could be enriched during the bauxitisation process. The LREE enrichment could be related to the differences in the mineral stability. The La, Ce and Pr accumulation could also be related to the prevalent physico-chemical conditions (Meen, 1990; Braun et al. 1998).

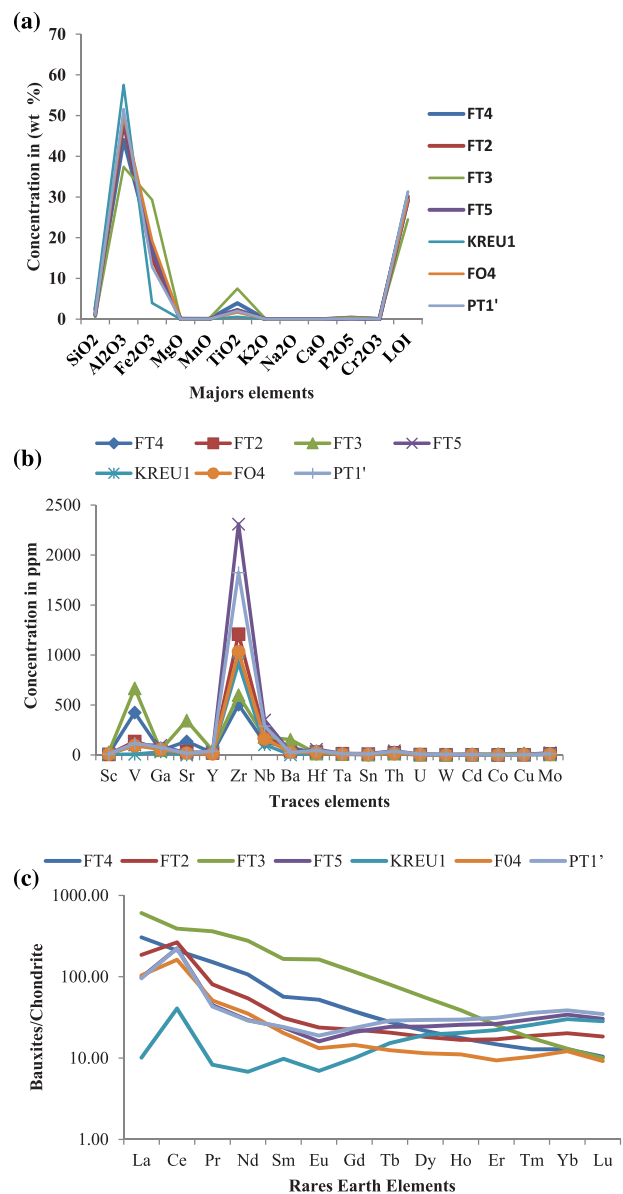


**Figure 16.** (a,b) The major and trace elements related variation, concerning the Fongo-Tongo lateritic bauxite. (c) Chondrites normalised rare-earth composition of the Fongo-Tongo lateritic bauxites (after McDonough and Sun 1995).

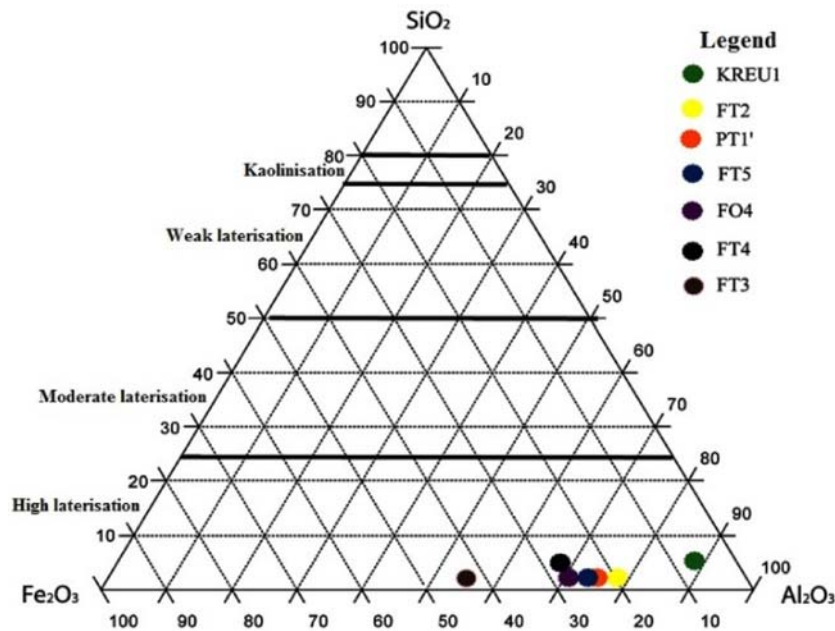


**Figure 17.** Fongo-Tongo bauxitic samples on the  $\text{SiO}_2\text{-Fe}_2\text{O}_3\text{-Al}_2\text{O}_3$  ternary diagram after Schellmann (1986).

The data of the bauxite on the ternary diagram of Schellmann (1986) showed that the investigated Fongo-Tongo bauxitic materials are derived from an environment characterised by strong lateritisation (Figure 17). Their position in the ternary diagram after Mutakyahwa et al. (2003) (Figure 18) showed that they are bauxites class.

The bauxites could be used for diverse industrial applications as depicted in the industrial specifications on Table 3 (after Rusel 1999).

### Geochemical correlations

Figure 19 shows a positive correlation between  $\text{TiO}_2$  and uranium. Strong positive correlations exist also between Ta-Nb (Figure 20); Zr-Hf (Figure 21) and Ba-Sr (Figure 22). These diagrams suggested that  $\text{TiO}_2$  and other elements (U, Ta, Nb, Hf, Zr, Ba and Sr) have similar geochemical behaviour and were relatively stable during the process of bauxitisation (Liu et al. 2010). Aluminium showed a positive correlation with the heavy rare earths (Er, Yb, and Lu) (Table 4).

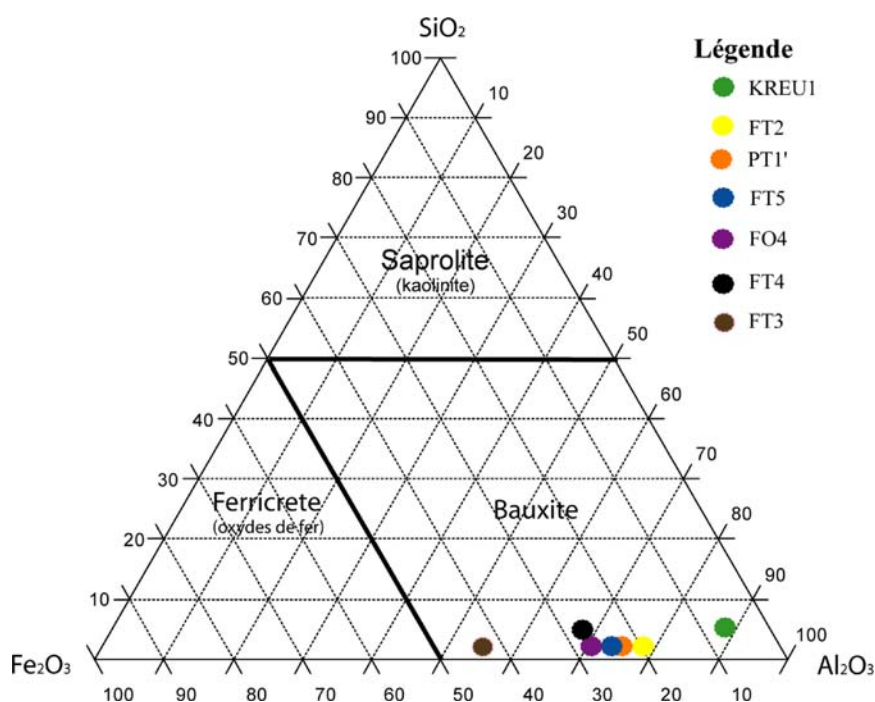


**Figure 18.** Fongo-Tongo bauxitic samples on the  $\text{SiO}_2\text{-Fe}_2\text{O}_3\text{-Al}_2\text{O}_3$  ternary diagram after Mutakyahwa et al. (2003).

**Table 3.** Classification of bauxites according to their respective uses.

	Bauxite used in the production of aluminium and alloys	Bauxite used in the elaboration of abrasive material	Bauxite used in the elaboration of refractory	Bauxite used in the production of chemical products/compounds	Bauxite used in cement composition
<b>Major oxides</b>	Al <sub>2</sub> O <sub>3</sub>	50–55	80–88	55–60	45–55
	SiO <sub>2</sub>	0–15	Max: 5	Max: 5–18	Max: 6
<b>%</b>	Fe <sub>2</sub> O <sub>3</sub>	5–30	2–5	Max: 2	20–30
	TiO <sub>2</sub>	0–6	2–4	Max: 4	3
<b>Corresponding bauxite</b>	FT5, FO4, PT1			KREU1	FT4, FT2

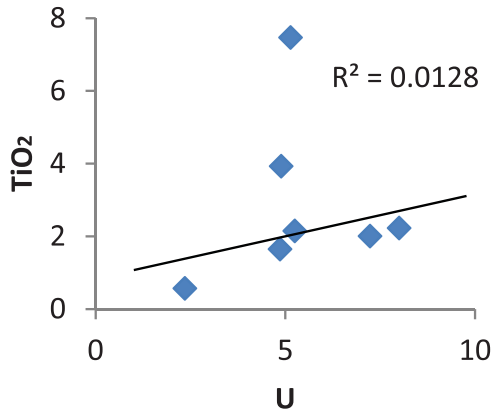


**Figure 19.** TiO<sub>2</sub> – U Binaire diagram.

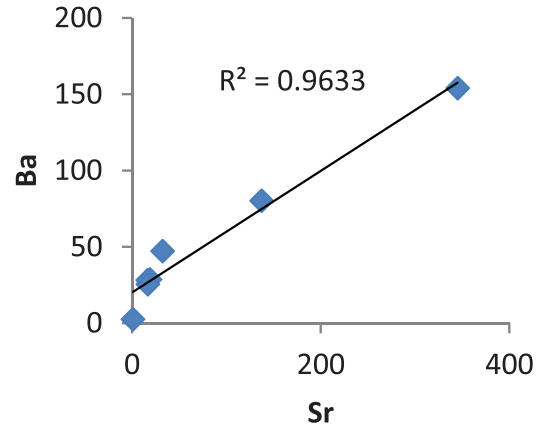


**Figure 22.** Ba–Sr Binaire diagram.

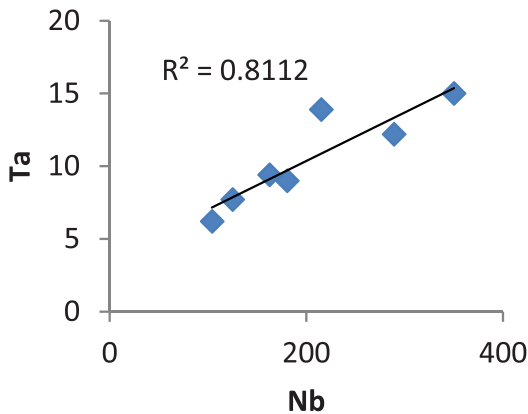


**Figure 20.** Ta–Nb Binaire diagram.

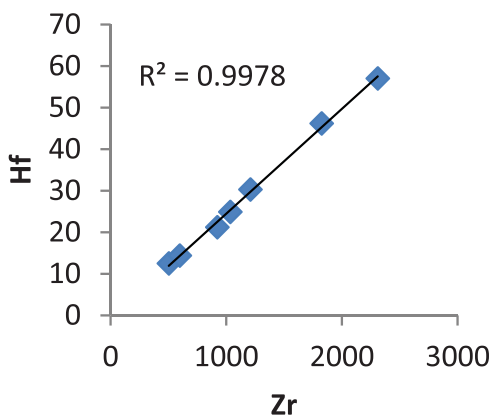


**Figure 21.** Hf–Zr Binaire diagram.

In addition, the positive correlations between heavy REE, zirconium and aluminium indicated that they are generally accompanied by minerals containing the Zr and Al (Esmaily et al. 2010).

The varied geochemical pattern observed in the analysed samples suggested either a difference in the degree of maturation or evolution of the alteration facies developed on the same parent rock or different parent rocks (acid to basic rock). The rate and duration of the weathering process of these materials may have varied in space and time with respect to fluctuations in paleoclimates, which occurred in the region of Fongo-Tongo. Variations in the major, trace and rare-earth elements are depicted in Figure 16(a–c), respectively.

**Parent rocks and weathering process in Fongo-Tongo area**

The rock types mapped in Fongo-Tongo area include the granite-gneiss basement, aphyritic basalts,

**Table 4.** Correlation coefficients of rare earth, major and traces.

	TiO <sub>2</sub>	P <sub>2</sub> O <sub>5</sub>	Sc	Al <sub>2</sub> O <sub>3</sub>	Nb	Zr
<b>La</b>	0.988	0.944	0.953			
<b>Ce</b>	0.851	0.712	0.749			
<b>Pr</b>	0.987	0.935	0.975			
<b>Nd</b>	0.984	0.928	0.98			
<b>Sm</b>	0.979	0.9	0.982			
<b>Eu</b>	0.976	0.896	0.983			
<b>Tb</b>	0.945	0.793	0.947			
<b>Er</b>	0.153		0.121	0.042	0.586	0.524
<b>Yb</b>				0.631	0.624	0.799
<b>Lu</b>				0.664	0.581	0.771

ignimbrites and trachytes (Figure 3). The amount of elements in the source rock and the chemical association of specific elements usually govern the chemical composition of bauxite deposit formed with stable and unstable minerals during weathering. Other contributing factors include the intensity of drainage during weathering, precipitation in situ (relative enrichment), vertical or ground water transport of elements (absolute enrichment). Besides aluminium, several elements, such as, Fe may be enriched to form important ore deposits.

The early stages of Fongo-Tongo basalt weathering have not been studied. However, the observations made in some exposures, such as, quarries showed that, from the early stages of weathering, rounded fragments formed are similar to those of trachyte. These observations are in agreement with the descriptions made by Belinga (1972) for the alteration of basalts and dolerites which formed the Adamaoua bauxites.

According to Laplaine (1969), Fongo-Tongo's bauxites are located on the ancient basalts that topographically rest on the trachytes of the Bam-boutos massif. According to Hiéronymus (1973), Fongo-Tongo's bauxitic formations are the result of the lateritic alteration of basalts, as well as trachytes.

Nyobe (1987) noted that the Fongo-Tongo bauxitic deposit on the western flank of Fongo-Tongo is on the Fondjoumetah. Those on the north-eastern flank is on the Melan, and Djeu sites, which indicated that the bauxite deposits in the Fongo-Tongo sector originated from the Tertiary lava flows in the area.

## Conclusions

The Fongo-Tongo area is characterised by three major geomorphological units occurring in a step-like manner, lying at an average altitude of 1500–1650 m. This corresponds to the bauxite deposits zone. The lateritic bauxite outcrops lie in the form of slabs and discontinuous blocks. This lateritic bauxite varies in shape from massive, vesicular, cellular and conglomeratic to nodular. These indurated materials have various colours that ranged from reddish, brick-red to reddish brown, brownish, pinkish, yellowish and ochre. Some have spots and purple frames, while others are mottled and greenish.

The mineralogical assemblage of these indurated materials showed that they are principally made up of gibbsite, subordinate goethite, with traces of quartz, anatase, hematite, maghemite and kaolinite.

Geochemical analysis reveals that these materials have high content of alumina and iron oxide while other oxides are low. The bauxites has significant contents of trace and rare-earth elements, notably Zr (504–2310), Nb (104–350), Sr (0.7–345), V (8–667), Y (24.9–239), La (2.4–144) and Nd (3.1–126) ppm.

However, the geochemical data from the Kreu lateritic bauxite located west of Fongo-Tongo, shows that this bauxite has the highest content in alumina (57.5%), and low concentration of impurities such as SiO<sub>2</sub> (3.21), Fe<sub>2</sub>O<sub>3</sub> (3.97 wt-%) and Zr (923), Nb (104), Sr (0.7), V (8.0), Ce (24.9) La (2.4) and Nd (3.1) ppm suggesting that the Fongo-Tongo lateritic bauxites are suitable as industrial raw material. It is important to note that further research is required to evaluate in detail the potential of the bauxite deposit as well as other relevant feasibility, environmental impact and most appropriate mining design for the sustainable exploitation of the deposit.


## Acknowledgements

The authors are indebted to Dr André NJOYA for his help during the sample preparation. We are extremely grateful to the reviewers and the Editor for their comments which significantly enhanced the quality of the manuscript.

## Disclosure statement

No potential conflict of interest was reported by the author(s).

## ORCID

Franck Wilfried Nguimatsia Dongmo  <http://orcid.org/0000-0001-7666-2455>

## References

- Akayemov ST, Pastukhova MV, Tenyakov VA, Yasamanov NA. 1975. Time and circumstances of bauxite formation from the lateritic crusts of the Earth's equatorial zone. In: Problems of bauxite genesis. Moscow: Izd. Nauka; p. 55–78.
- Bardossy G. 1982. Karst bauxites (Bauxite deposits on carbonate rocks) Budapest. Hungary.
- Bardossy GY, Aleva GJJ. 1990. Lateritic bauxites: developments in economic geology, vol. 27. Amsterdam: Elsevier Scientific Publication, 624 pp.
- Bardossy GY, Combes PJ. 1999. Karst bauxites: interfingering of deposition and palaeoweathering. Special Publications, 27. Blackwell Science, Alden Press; p. 189–206. doi:10.1002/9781444304190.ch7
- Belinga SE. 1972. *L'altération des roches basaltiques et le processus de bauxitisation dans l'Adamaoua (Cameroun)*. (Ph. D. thesis, University of Paris VI, Paris).
- Belinga SME. 1972. *L'altération des roches basaltiques et le processus de bauxitisation dans l'Adamaoua (Cameroun)* (Doctoral dissertation, Verlag nicht ermittelbar).
- Bineli Betsi TO. 2002. Les formations bauxites de la région de Fouban (Ouest – Cameroun): Etude préliminaire. Mém. DEA, Univ. Ydé I, 88p.
- Boulangé B. 1984. *Les formations bauxitiques latéritiques de Côte d'Ivoire: les faciès, leur transformation, leur distribution et l'évolution du modelé*. Travaux et Documents de l'ORSTOM, (175).
- Braun JJ, Viers J, Drupé B, Polve M, Ndam J, Muller JP. 1998. Solid/liquid REE.
- Brindley GW, Brown G. 1980. Quantitative X-ray mineral analysis of clays. Crystal structures of clay minerals and



- their X-ray identification. Vol. 5, 411–438. doi:10.1180/mono-5.7
- Déruelle B, Moreau C, Nkoumbou C, Kambou R, Lissom J, Njonfang E, Ghogomu RT, Nono A. 1991. The Cameroon line: a review. In: *Magmatism in extensional structural settings*. Berlin: Springer; p. 274–327.
- Dumort JC. 1968. Carte géologique de reconnaissance à l'échelle du 1/500 000. Notice explicative sur la feuille de Douala-Ouest. B.R.G.M., Dir. Min. Géol. Cam., 69 p.
- Esmaeily D, Rahimpour-Bonab H, Esna-Ashari A, Kananian A. 2010. Petrography and geochemistry of the Jajarm bauxite ore deposit, Northeast Iran: implications for source rock material and Ore Genesis. *Turkish Journal of Earth Sciences*. 19(2):267–284.
- Grubb PLC, PLC G. 1973. High-level and low-level bauxitization: a criterion for classification.
- Hiéronymus B. 1973. Etude minéralogique et géochimique des formations bauxitiques de l'Ouest du Cameroun. *Cahiers ORSTOM. Série Géologie*. 5(1):97–112.
- Kanga MA. 2012. Etude géologique des indices bauxitiques du secteur de Bangam (Ouest-Cameroun). Mémoire Master, Fac. Sci., Université Yaoundé I. 96.
- Laplaine L. 1969. Indices minéraux et ressources minérales du Cameroun et synthèse simplifiée des connaissances sur la géologie du Cameroun.
- Liu X, Wang Q, Deng J, Zhang Q, Sun S, Meng J. 2010. Mineralogical and geochemical investigations of the Dajia Salento-type bauxite deposits, western Guangxi, China. *J Geochem Explor*. 105(3):137–152. doi:10.1016/j.gexplo.2010.04.012.
- McDonough WF, Sun SS. 1995. The composition of the earth. *Chem Geol*. 120(3-4):223–253. doi:10.1016/0009-2541(94)00140-4.
- Meen JK. 1990. Negative Ce anomalies in Archean amphibolites and Laramide granitoids, southwestern Montana, USA. *Chem Geol*. 81(3):191–207. doi:10.1016/0009-2541(90)90115-N.
- Momo Nouazi M, Tematio P, Yemefack M. 2012. Multi-Scale Organization of the Doumbouo-Fokoué bauxite Ore deposits (west Cameroun): Implication to the landscape Lowering. *Open Journal of Geology*. 2:14–24. doi:10.4236/ojg.2012.21002.
- Moore DM, Reynolds Jr RC. 1989. X-ray diffraction and the identification and analysis of clay minerals. Oxford University Press (OUP).
- Morin S. 1988. Les dissymétries fondamentales des hautes terres de l'Ouest-Cameroun et leurs conséquences sur l'occupation humaine: Exemple des monts Bambouto. *L'homme et la montagne tropicale*. Sepanrit ed., Bordeaux, 49–51.
- Mutakyahwa MKD, Ikingura JR, Mruma AH. 2003. Geology and geochemistry of bauxite deposits in Lushoto District, Usambara mountains, Tanzania. *J Afr Earth Sci*. 36(4):357–369. doi:10.1016/S0899-5362(03)00042-3.
- Nguimatsia DFW. 2013. Contribution à l'étude géologique des formations bauxitiques de Fongo-Tongo (OUEST-CAMEROUN); *Mémoire Master, Fac. Sci., Université Yaoundé I*, 107, *laboratoire de Géologie appliquée - métallogénie, option: géologie minière*.
- Nguimatsia DFW, Yongue RF, Bolarinwa AT, Ngatcha RB, Fuanya C, Kanga MA. 2019. Contribution to the Study of Bauxites' Formation in the Fongo-Tongo (Western Cameroon) Sites. In *Petrogenesis and Exploration of the Earth's Interior* (pp. 241–244). Springer, Cham. doi:10.1007/978-3-030-01575-6\_58.
- Njonfang E, Nono A, Kamgang P, Ngako V, Tchoua FM. 2011. Cameroon line alkaline magmatism (Central Africa): a reappraisal. *Geological Soc America Special Paper*. 478:173–192. doi:10.1130/2011.2478(09).
- Nni J, Nyobe JB. 2011. Géologie et pétrologie des laves précaldériques des Monts Bambouto: ligne du Cameroun. *Geochimica Brasiliensis*. 9(1).
- Nyobe JB. 1987. A geological and geochemical study of the Fongo Tongo and areally related bauxite deposits, Western Highlands, Republic of Cameroon. Doc. Ph.D., Lehigh Univ., 352 p.
- Price GD, Valdes PJ, Sellwood BW. 1997. Prediction of modern bauxite occurrence: implications for climate reconstruction. *Palaeogeogr Palaeoclimatol Palaeoecol*. 131(1-2):1–13. doi:10.1016/S0031-0182(96)00145-9.
- Rusel A, et al. 1999. Bauxite and alumina. A guide to non-met-allurgical uses and markets. Industrial mineral information limited, park house, park terrace, surrey KT47HY.UK ISBN: 1900663619. 129p.
- Sato H, Aramaki S, Kusakabe M, Hirabayashi JI, Sano Y, Nojiri Y, Tchoua F. 1990. Geochemical difference of basalts between polygenetic and monogenetic volcanoes in the central part of the Cameroon volcanic line. *Geochem J*. 24(6):357–370. doi:10.2343/geochemj.24.357.
- Schellmann W. 1986. A new definition of laterite. *Memoirs of the geological survey of India. Journal of African Earth Science*. 120:1–7.
- Schwertmann U, Murad E. 1983. Effect of pH on the formation of goethite and hematite from ferrihydrite. *Clays Clay Miner*. 31(4):277–284. doi:10.1346/CCMN.1983.0310405.
- Ségalen P. 1964. Le fer dans les sols. *Init. Doc. Tech., ORSTOM*, Paris, 4, 150 p.
- Sojien M. 2007. Etude pétrographique, minéralogique et géochimique des formations bauxitiques de Bangam dans les hautes terres de l'Ouest – Cameroun. *Mém. Master, Univ. Dschang*, 77 p.
- Tardy Y. 1993. *Pétrologie des latérites et des sols tropicaux*. Masson, Paris, 461 p.
- Tardy Y, Kobilsek B, Paquet H. 1991. Mineralogical composition and geographical distribution of African and Brazilian periatlantic laterites. The influence of continental drift and tropical paleoclimates during the past 150 million years and implications for India and Australia. *J African Earth Sciences (and the Middle East)*. 12(1-2):283–295. doi:10.1016/0899-5362(91)90077-C.
- Tchoua F. 1974. *Contribution à l'étude géologique et pétrologique de quelques volcans de la ligne du Cameroun (Monts Manengouba et Bambouto)* (Doctoral dissertation, Sc. nat.: Clermont Ferrand: 1974; E, 187.).
- Valeton I. 1972. *Bauxites*. Amsterdam: Elsevier Publishing Company, 226 pp.
- Valeton I. 1999. Saproliite-bauxite facies of ferralitic duricrusts on palaeosurfaces of former Pangaea. doi:10.1002/9781444304190.ch6
- Yongue Fouateu R. 1986. Contribution à l'étude pétrologique de l'altération et des faciès de cuirassement ferrugineux des gneiss migmatiques de la région de Yaoundé. *Thèse Doct. 3<sup>e</sup> Cycle, Univ. Yaoundé I*, 214 p.
- Youmen D. 1994. Evolution volcanologique, pétrologique et temporelle de la caldeira des Monts Bambouto (Cameroun). *Thèse Univ. Christian albrecht Kiel, Allemagne*, 274 p. + 2 cartes.

## Appendices

### Appendix 1. General characteristics of the main Bauxite deposits in Cameroon

Region	Locality		Al <sub>2</sub> O <sub>3</sub>	SiO <sub>2</sub>	Fe <sub>2</sub> O <sub>3</sub>	Altitude (m)	Surface (Km <sup>2</sup> )	Strength (m)	Stocks (Mt)	Protolith	Morphology	
Adamaoua plateau	Minim-Martap	A	48,6	1,8	-	1200–1300	-	-	1500	Basalt	Tabular relief	
		A	46,3	1,8	-	-	-	-	-	-	-	
	Ngaoundal Ngaoundourou	A	-	-	-	1200–1400	-	-	-	-	-	
Western highlands	Fongo Tongo	B	40,0–53,0	2,0–3,6	20,0–30,0	-	-	5–11	45	Basalt/ Trachyte	Tabular relief	
		C	39,0	25,2	14,1	1650	-	-	46	-	-	
		D	33,3–60,5	1,0–5,0	-	-	-	-	9–10	-	Trachyte	-
		E	37,4–57,5	0,48–3,21	3,97–29,3	1300–1650	-	-	-	-	-	Wavy relief
		B	41,0–46,0	4,3–8,0	-	1400–2000	-	-	-	4	Trachyte	-
	Southern parts of the mountains Bangam	I	20–50,80	1,28–5,76	14–47,6	-	-	-	-	-	Basalt	Wavy relief
		C	47,8	0,6	20,1	-	-	4–5	-	-	Basalt	-
		F	38,4–60,4	2,6–22,4	9,1–42,3	1500–1700	7,4	3–5	-	-	Basalt	-
		A	40,0	2,0	-	-	-	3–5	-	-	-	-
		F	52,0–61,0	0,5–1,0	8,0–13,0	1100–1200	-	4–9	-	-	Basalt/ Trachyte	-
Doumbouo-Fokoué	G	47,5–49,5	1,8–7,6	20,0–22,0	-	5,7	10–12	9,2	Basalt	-		

#### Legend:

A: datas obtained by Belinga (1972) F: datas obtained by Sojien (2007)  
 B: datas obtained by Belinga (1972) G: datas obtained by Bineli Betsi (2002)  
 C: datas obtained by Hiéronymus (1973) H: datas obtained by Momo Nouazi et al. (2012)  
 D: datas obtained by Nyobe (1987) I: datas obtained by Kamga (2012)  
 E: datas obtained by Nguimatsia (2013) Mt: Million tones

**Appendix 2. Photography of samples submitted to geochemical and mineralogical analyses.**



**FT5**



**PT1'**



**FT3**



**FO4**



**Kreu1**



**FT4**



**FT2**



**FT1**

**Appendix 3: Inventory and location of samples taken in the locality of Fongo-Tongo**

Samples	GPS	Locations	Altitudes
FT5	5° 30'53" 9° 58'46"	Nzie-fonda	1584m
PT <sub>1</sub>	5° 31'46" 9° 58'33"	Leuke-zack	1666m
PT <sub>1'</sub>	5° 31'46" 9° 58'33"	Leuke-zack	1671m
FO <sub>1</sub>	5° 31'57" 9° 59'10"	Meza	1658m
FO <sub>1-2</sub>	5° 31'55" 9° 59'09"	Meza	1637m
FO <sub>2</sub>	5° 31'47" 9° 59'20"	Meza	1646m
FO <sub>3</sub>	5° 31'33" 9° 59'21"	Lepooh	1610m
FO <sub>4</sub>	5° 31'29" 9° 59'16"	Lepooh	1634m